

# Reaction and characterization studies of an industrial Cr-free iron-based catalyst for high-temperature water gas shift reaction

Quansheng Liu<sup>\*</sup>, Wenping Ma<sup>1</sup>, Runxia He, Zhanjun Mu

*Department of Chemical Engineering, Inner Mongolia University of Technology, Hohhot 010062, PR China*

Available online 22 August 2005

## Abstract

Activity and stability of an industrial Cr-free iron-based catalyst (NBC-1) for high-temperature water gas shift (WGS) reaction were studied in a fixed-bed reactor under 350 °C, 1 atm, H<sub>2</sub>O:gas = 1:1 and 3000 h<sup>-1</sup> (dry-gas basis). Physical properties of the NBC-1 catalyst before and after the WGS reaction, the desorption behavior of H<sub>2</sub>O, CO, CO<sub>2</sub> and H<sub>2</sub>, and surface reaction over the catalyst were characterized by BET, X-ray diffraction (XRD), Mössbauer emission spectroscopy (MES), temperature programmed desorption (TPD) and temperature programmed surface reaction (TPSR). The NBC-1 catalyst is active and has excellent thermo-stability even after pretreatment at a high temperature of 530 °C. Its activity and thermo-stability are comparable to those of an UCI commercial Fe-Cr catalyst, C12-4. XRD and MES studies show that iron in the fresh NBC-1 catalyst is present as  $\gamma$ -Fe<sub>2</sub>O<sub>3</sub>, most of which is converted to Fe<sub>3</sub>O<sub>4</sub> during reduction and reaction. Results of TPD demonstrate that adsorbed CO<sub>2</sub> and CO cannot exist on the NBC-1 surface beyond the temperature of 300 °C while higher temperatures (>400 °C) are required to completely desorb H<sub>2</sub>O. A redox mechanism of WGS on the NBC-1 surface is proposed based on the TPD and TPSR observations.

© 2005 Elsevier B.V. All rights reserved.

**Keywords:** Water gas shift reaction;  $\gamma$ -Fe<sub>2</sub>O<sub>3</sub>; Fe<sub>3</sub>O<sub>4</sub>; Cr-free; Redox mechanism

## 1. Introduction

Fe-Cr oxide catalysts have been used industrially for water gas shift reaction ( $\text{CO} + \text{H}_2\text{O} = \text{CO}_2 + \text{H}_2$ ) in the high temperature range of 320–480 °C. This type of catalyst has demonstrated high WGS activity and excellent thermo-stability, probably because the Cr promoter acts as a structural stabilizer and/or a structure promoter [1,2]. However, it has been found that commercial iron-based WGS catalysts with as high as 8–14 wt% Cr promoter generally contain about 2 wt% Cr<sup>6+</sup> compound, which is highly toxic to humans and environment during its manufacture and deposition [1,3–6]. Thus, it has drawn considerable attention to study Cr-free iron-based WGS catalysts in past years.

Various kinds of oxides have been employed, e.g., PbO, La<sub>2</sub>O<sub>3</sub>, CaO, ZrO<sub>2</sub>, Al<sub>2</sub>O<sub>3</sub>, etc., to replace Cr<sub>2</sub>O<sub>3</sub> in order to achieve practical Cr-free Fe-based WGS catalysts [3,5,7–10]. Shirokov [7] studied PbO promoted iron WGS catalyst. When the content of PbO promoter is optimized to around 10%, the Fe-Pb-based catalyst shows similar catalytic performance to that of a commercial Fe-Cr-based WGS catalyst, C12-4, manufactured by United Catalyst Inc. (UCI). However, the stability of the Fe-Pb-based catalyst is incomparable since its activity is sensitive to trace amount of sulfur in the water-gas feedstock. By using the oxides of Ca, Sr, Ba or Zr, Imperial Chemical Industries (ICI) made a series of Cr-free iron-based WGS catalysts [3]. It was found that the activity of these catalysts was extremely low. Other investigators compared the roles of ThO<sub>2</sub>, MnO<sub>2</sub>, MgO and Al<sub>2</sub>O<sub>3</sub> in the iron catalyst [5,8–10] and reported that Al<sub>2</sub>O<sub>3</sub> could enhance catalyst stability to some extent. In recent years, studies show that Ceria is promising for the high WGS reaction [11–14]. It was reported that the Ce promoter increases the reducibility of metals and inhibits metal

<sup>\*</sup> Corresponding author. Tel.: +86 471 6576154; fax: +86 471 6575796.

E-mail addresses: [liuqs@imut.edu.cn](mailto:liuqs@imut.edu.cn) (Q. Liu),  
[wen-ping.ma@mail.wvu.edu](mailto:wen-ping.ma@mail.wvu.edu) (W. Ma).

<sup>1</sup> Present address: Department of Chemical Engineering, West Virginia University, Morgantown, WV 26506-6102, USA.

sintering [13,15]. Most recently, some groups reported that addition of CeO<sub>2</sub> to Fe-Cr- and Cr-free iron- and Cu-based WGS catalysts effectively modified catalyst performance [5,13,16].

There are at least two challenges in preparing Cr-free iron-based WGS catalyst that is to maintain catalyst activity and thermo-stability. It has been realized that activity and thermo-stability of the iron catalyst is corrected with crystal structure of iron oxides such as  $\alpha$ -Fe<sub>2</sub>O<sub>3</sub> and  $\gamma$ -Fe<sub>2</sub>O<sub>3</sub> [6,17].  $\gamma$ -Fe<sub>2</sub>O<sub>3</sub> was found to be more active for the WGS reaction than  $\alpha$ -Fe<sub>2</sub>O<sub>3</sub>, since the activation energy of the former phase is less than that of the latter [17]. On the other hand, the crystal of  $\gamma$ -Fe<sub>2</sub>O<sub>3</sub> generally possesses an imperfect cubic spinel structure, which is different from that of  $\alpha$ -Fe<sub>2</sub>O<sub>3</sub>, hexagonal structure. The imperfect spinel of  $\gamma$ -Fe<sub>2</sub>O<sub>3</sub> allows promoters such as Cr or Ce to be incorporated into vacant sites in the  $\gamma$ -Fe<sub>2</sub>O<sub>3</sub>, resulting in less sintering of active phase in the catalysts consisting of  $\gamma$ -Fe<sub>2</sub>O<sub>3</sub> than those containing  $\alpha$ -Fe<sub>2</sub>O<sub>3</sub> under identical operating conditions [6]. To this end, it is very important to form as much  $\gamma$ -Fe<sub>2</sub>O<sub>3</sub> as possible during preparation of Cr-free iron-based WGS catalyst. However, information about doing this is limited.

We prepared an industrial Cr-free iron catalyst promoted by oxides of Ce and Al according to the method described elsewhere [18]. The formation of  $\gamma$ -Fe<sub>2</sub>O<sub>3</sub> is controlled successfully by adjusting core preparation parameters, namely the ratio of Fe<sup>2+</sup>/Fe<sup>3+</sup> in the iron solution and the proper aging time. The catalytic performance was studied in a bench-scale fixed-bed reactor. Physical properties (surface area and crystal phase) of the catalyst and surface reaction mechanism including the desorption behavior of CO, H<sub>2</sub>O and CO<sub>2</sub> and surface reaction of CO and H<sub>2</sub>O on the catalyst surface were studied through BET, X-ray diffraction (XRD), Mössbauer emission spectroscopy (MES), temperature programmed desorption (TPD) and temperature programmed surface reaction (TPSR).

## 2. Experimental

### 2.1. Catalyst synthesis

The commercial NBC-1 catalyst was prepared using the wet precipitation technique. Details of the preparation procedures were reported previously [18]. In brief, the NBC-1 catalyst was prepared by precipitation of iron sulfite with ammonia solutions (industrial grade) in an industrial precipitation vessel ( $D = 1450$  mm and  $H = 1850$  mm). Before precipitation, an iron sulfite solution in the vessel was partly oxidized by air until the desired amount of Fe<sup>3+</sup> cations (Fe<sup>2+</sup>/Fe<sup>3+</sup>  $\sim 2.0$ ) was achieved. Promoters of Al<sub>2</sub>O<sub>3</sub> and CeO<sub>2</sub> (in powder form) were added during precipitation. The resulting slurry was subsequently aged followed by washing, drying and calcination.

### 2.2. Fixed-bed reactor test

The activity of NBC-1 catalyst (12–14 mesh,  $\sim 2$  g) was examined in a bench-scaled fixed-bed stainless steel reactor (i.d. = 10 mm) under atmospheric pressure, 350 °C and 3000 h<sup>-1</sup> (dry-gas basis). The composition of the feed gas was 26% CO, 8% CO<sub>2</sub>, 40% H<sub>2</sub> and 26% N<sub>2</sub> (internal standard). Prior to the WGS reaction, the NBC-1 catalyst was reduced using the same reactant gas mixture under the severe conditions of 530 °C, 3000 h<sup>-1</sup> and 1 atm for 15 h. The gas composition before and after the WGS reaction was analyzed online by a GC-8A gas chromatograph (GC).

### 2.3. Catalyst characterization

The BET surface areas of the catalysts were measured by isothermal adsorption of N<sub>2</sub> at 77 K using a surface area porosity analyzer ASAP2010. All samples were degassed at 120 °C for 1 h prior to measurements.

XRD analysis of fresh and spent catalysts (spent catalyst was transferred to a small vial filled with inert gas after the run) was carried out using a Rigaku/max-RB X-ray diffraction meter and Cu K $\alpha$  radiation source (1.5418 Å).

MES measurement was conducted using a constant acceleration spectrometer named OXFORD-MS-500. The radioactive source consists of 25 mCi of <sup>57</sup>Co in a Pd matrix. The results were calibrated by the standard spectrum of  $\alpha$ -Fe foil with a thickness of 6  $\mu$ m and a purity of 99.59%. The absorption thickness is 7–8 mg Fe/cm<sup>2</sup> and the baseline-count per channel is (5–40)  $\times 10^5$ . Mössbauer data analysis was performed by least-square fitting of the 6-line or 12-line Mössbauer spectrum.

The desorption behavior and surface reaction of CO, H<sub>2</sub>O or CO<sub>2</sub> species on the catalyst surface were characterized by the TPD and TPSR, respectively, using a Micrometrics Autochem 2910 instrument. Before each experiment, the reduced NBC-1 catalyst was saturated by the CO, H<sub>2</sub>O or CO<sub>2</sub> molecular at room temperature (RT) for 1 h.

## 3. Results and discussion

### 3.1. BET and reaction results of the NBC-1 catalyst

Table 1 gives the bulk composition, BET surface areas of the fresh and spent NBC-1 catalyst along with activity ( $X_{\text{CO}}$ , %) of the catalyst at 350 °C. The same experimental data of a commercial Fe-Cr WGS catalyst denoted as C12-4, which is supplied by UCI, are also listed in Table 1 for comparison. The bulk Fe<sub>2</sub>O<sub>3</sub> content in the NBC-1 catalyst is slightly higher than that of the C12-4 catalyst (88.8% versus 81.2%). The BET surface areas of both catalysts before reaction are nearly the same (70–73 m<sup>2</sup>/g). After WGS reaction, the BET surface areas of NBC-1 and C12-4 catalysts are decreased by 52% (to 35.2 m<sup>2</sup>/g) and 42% (to 40.4 m<sup>2</sup>/g), respectively. CO conversions at 350 °C at steady state for both catalysts

Table 1  
Bulk and textural properties and activity of NBC-1 and C12-4 catalysts

Catalyst ID	Bulk composition (wt%) <sup>a</sup>	BET surface area (m <sup>2</sup> /g)		$X_{\text{CO}}$ (%) <sup>b,c</sup>
		Fresh catalyst	Spent catalyst	
NBC-1	88.6 Fe <sub>2</sub> O <sub>3</sub> /2.0 Al <sub>2</sub> O <sub>3</sub> /0.5 CeO <sub>2</sub>	72.8	35.2	53.0
C12-4	81.2 Fe <sub>2</sub> O <sub>3</sub> /8.8 Cr <sub>2</sub> O <sub>3</sub>	70.3	40.4	53.8

<sup>a</sup> Balanced by graphite and water.

<sup>b</sup>  $X_{\text{CO}}$  (%) = 100 × (CO mole flow rate in – CO mole flow rate out)/CO mole flow rate in.

<sup>c</sup> Values were measured under 350 °C, 1 atm, H<sub>2</sub>O:gas = 1:1 and 3000 h<sup>–1</sup> (dry-gas basis: 26% CO, 8% CO<sub>2</sub>, 40% H<sub>2</sub> and 26% N<sub>2</sub>) after catalysts were kept at 530 °C for 15 h by flowing the reactant gas.

are high and nearly the same (53–54%), which is qualitatively consistent with their surface areas after the runs. Note that the catalytic activity of the two commercial catalysts was measured after the catalysts experienced severe thermo-resistance test during the reduction period (530 °C and 15 h). The high CO conversions indicate that both catalysts have excellent thermo-resistance behavior.

### 3.2. XRD and MES studies of the NBC-1 catalyst

The XRD patterns of the fresh and spent NBC-1 catalyst are presented in Fig. 1a and b. The eight peaks centered at 21.3°, 25.4°, 30.3°, 35.6°, 43.5°, 53.9°, 57.2° and 62.7° in the XRD pattern of the fresh catalyst (Fig. 1a) correspond well to the reference data of  $\gamma$ -Fe<sub>2</sub>O<sub>3</sub> spinel structure. The lattice parameter of  $\gamma$ -Fe<sub>2</sub>O<sub>3</sub> crystalline structure, as obtained from the peak positions present in Fig. 1a is 8.35 Å. For the pattern of the spent catalyst, the seven peaks occurred at 17.3°, 29.8°, 35.5°, 43.1°, 53.4°, 57.0° and 62.5° represent the reflection characteristic of the Fe<sub>3</sub>O<sub>4</sub> spinel (Fig. 1b), and its lattice parameter of Fe<sub>3</sub>O<sub>4</sub> crystalline structure is 8.40 Å. One peak (at 2 $\theta$  of 26.1°) in Fig. 1b does not fit Fe<sub>3</sub>O<sub>4</sub>, but a new kind of iron oxide phase is probably formed. The XRD result demonstrates that the fresh NBC-1 catalyst is

primarily made up of  $\gamma$ -Fe<sub>2</sub>O<sub>3</sub>, and most of it is converted to Fe<sub>3</sub>O<sub>4</sub> during reduction and reaction. No Al and Ce crystalline phases (oxide or metallic) are observed in the XRD patterns of the fresh and spent catalyst. This likely indicates that the Al and Ce precursors are highly dispersed in the catalyst.

The Mössbauer spectra of the fresh and spent NBC-1 catalyst are shown in Fig. 2a and b, respectively. The MES spectra were fitted by a distribution of hyperfine fields, following the Hesse–Rubartsch algorithm. The corresponding best-fit parameters, i.e., isomer shift (IS), quadrupole splitting (QS) and hyperfine field ( $H_{\text{hf}}$ ) are summarized in Table 2. The spectrum of the fresh catalyst (Fig. 2a) consists of a typical sextet with isomer shift of about 0.32 and a hyperfine field of 49 T, which arises from the magnetic static regime of  $\gamma$ -Fe<sub>2</sub>O<sub>3</sub> [19]. The spectrum of the spent catalyst (Fig. 2b) shows two sextets with different isomer shifts (0.27 versus 0.65) and hyperfine fields (49 T versus 46 T), which arises from magnetite [8,20]. The MES results are quite consistent with the XRD results discussed above. Further, analysis of the Mössbauer spectrum of the spent catalyst

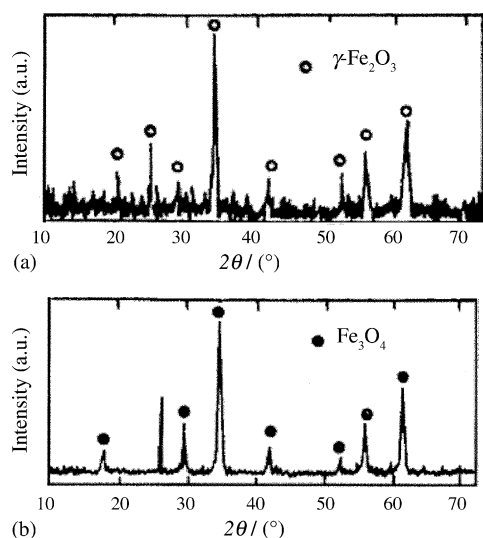


Fig. 1. XRD patterns (a) fresh NBC-1 catalyst and (b) spent NBC-1 catalyst.

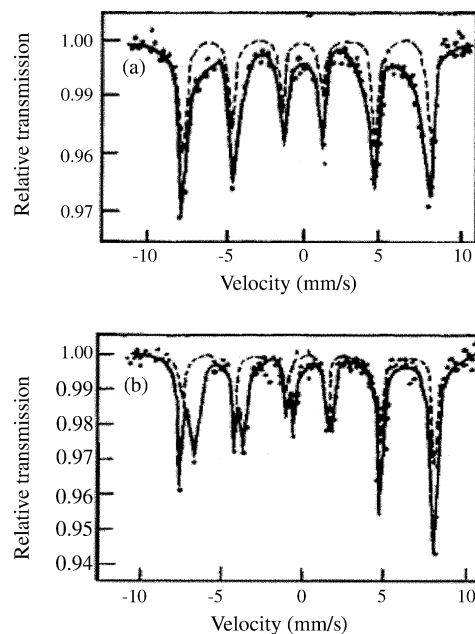


Fig. 2. MES patterns (a) fresh NBC-1 catalyst and (b) spent NBC-1 catalyst.

Table 2  
Parameters of Mössbauer spectra of the fresh and spent NBC-1 catalyst

NBC catalyst	IS (mm/s)	QS (mm/s)	$H_{\text{hf}}$ (T)	Area (%)	Area <sub>B</sub> /area <sub>A</sub>	Structure
Fresh	0.32	0.00	49.0	–	–	$\gamma\text{-Fe}_2\text{O}_3$
Spent						
Tetrahedral (A) site	0.27	−0.01	48.8	32	2.0	$\text{Fe}_3\text{O}_4$
Octahedral (B) site	0.65	−0.01	45.7	64		

IS, isomer shift; QS, quadrupole splitting;  $H_{\text{hf}}$ , hyperfine field.

shows that the relative ratio of the population of Fe at B-site (octahedral site) to that at A-site (tetrahedral site) is equal to the stoichiometric value of  $\text{Fe}_3\text{O}_4$  (2.0), indicating the structure of the  $\text{Fe}_3\text{O}_4$  after reduction or reaction is perfect.

### 3.3. Desorption and surface reaction on the NBC-1 catalyst

The  $\text{H}_2\text{O}$ -,  $\text{CO}_2$ - and  $\text{CO}$ -TPD profiles for the NBC-1 catalyst were illustrated in Fig. 3a–c. Two  $\text{H}_2\text{O}$  desorption peaks appear in the  $\text{H}_2\text{O}$ -TPD profile (Fig. 3a). The first

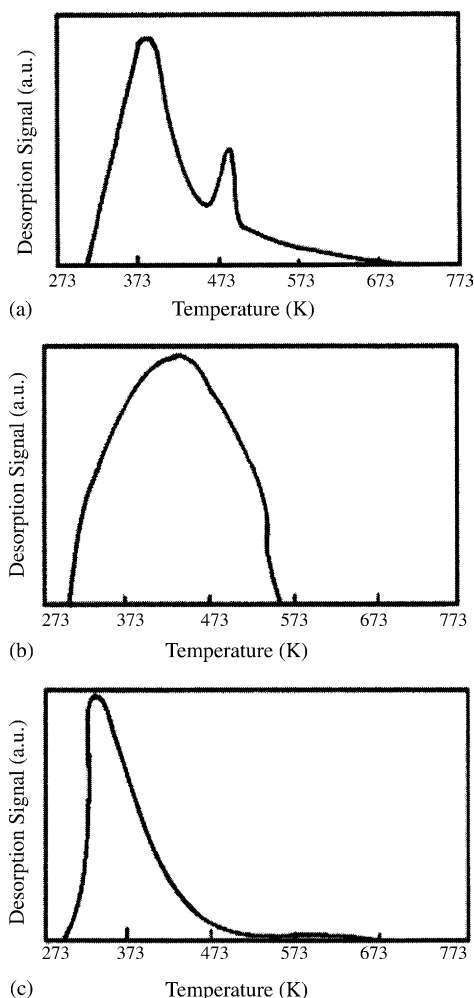


Fig. 3. TPD profiles of (a)  $\text{H}_2\text{O}$ , (b)  $\text{CO}_2$  and (c)  $\text{CO}$  on the NBC-1 catalyst.

large peak located between 300 and 470 K is assigned to desorption of physisorbed water on the catalyst. The second peak occurring between 470 and 673 K is ascribed to the desorption of chem-adsorbed water on the NBC-1 surface. It is interesting that only one large  $\text{CO}_2$  desorption peak is observed between 300 and 570 K (Fig. 3b). This indicates that the NBC-1 catalyst has a high capacity of reserving  $\text{CO}_2$  at RT; the adsorbed  $\text{CO}_2$  can be desorbed completely from the catalyst surface at about 570 K. Fig. 3c shows a small  $\text{CO}$  desorption peak. The maximum  $\text{CO}$  desorption signal occurs at around 373 K, and  $\text{CO}$  is not detected beyond 500 K.

In view of these observations, we may picture the desorption behavior of the adsorbed  $\text{H}_2\text{O}$ ,  $\text{CO}$  and  $\text{CO}_2$  at 350 °C on the NBC-1 catalyst. It is impossible that the adsorbed  $\text{CO}$  exists on the catalyst surface at this temperature since the  $\text{CO}$  desorption signal cannot be seen. In this case,  $\text{CO}$  must be in gas phase to participate the WGS reaction. A part of  $\text{H}_2\text{O}$  might be in the adsorbed state at 350 °C because the adsorbed  $\text{H}_2\text{O}$  is completely desorbed after 500 °C (773 K). Generally, the WGS reaction is interpreted by two prevailing mechanism models, i.e., the redox regenerative model and the associative model [1,8,21,22]. In the redox regenerative model, it is assumed that the catalyst surface is oxidized and reduced by  $\text{CO}$  and adsorbed  $\text{H}_2\text{O}$ ; an active oxygen specie is produced on the surface of the metal oxide by dissociation of adsorbed  $\text{H}_2\text{O}$ ,  $\text{H}_2\text{O}(\text{ads}) \leftrightarrow \text{H}_2(\text{g}) + \text{O}(\text{ads})$ , and oxygen vacancies in the metal oxide act as an adsorption site for  $\text{H}_2\text{O}$ ;  $\text{CO}_2$  is produced via  $\text{CO}$  reacting with an O site dissociated from  $\text{H}_2\text{O}$  [21]. In the associative model, it is assumed that  $\text{CO}_2$  and  $\text{H}_2$  are produced through formate species formed by adsorbed  $\text{CO}$  and  $\text{H}_2\text{O}$  [22]. Thus, the current TPD result is consistent with the redox regenerative mechanism. Further,  $\text{CO}_2$  is desorbed easily below 570 K (Fig. 3b), which is not consistent with a slow step of  $\text{CO}_2$  formation assumed in the associative mechanism. This may further indicate that the redox mechanism is a dominant pathway for the WGS reaction on the NBC-1 surface. This result is in agreement with the studies on iron-based WGS catalysts reported in [4], [8] and [21].

The reduced NBC-1 catalyst adsorbed  $\text{H}_2\text{O}$  at RT for 1 h, followed by the TPSR of  $\text{H}_2\text{O}$  and  $\text{CO}$  between RT and 773 K (3 K/min). A gas mixture of 5% $\text{CO}/\text{N}_2$  was used for the TPSR.  $\text{H}_2$  effluent was monitored by a GC with a TCD.

Fig. 4 shows the result of the TPSR of  $\text{H}_2\text{O} + \text{CO}$  on the NBC-1 catalyst.  $\text{H}_2$  signal starts at 513 K, suggesting the

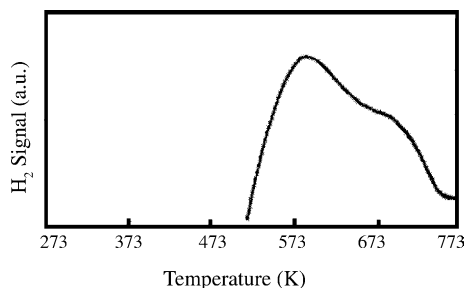


Fig. 4. TPSR profile of H<sub>2</sub>O and CO on the NBC-1 catalyst.

onset of the surface reaction between the adsorbed H<sub>2</sub>O and CO (Fig. 4). The amount of H<sub>2</sub> goes up with temperatures and peaks at about 573 K. As discussed above, part of the adsorbed H<sub>2</sub>O exists on the catalyst surface at 513 K. With increasing temperature, two possible reactions take place for the adsorbed H<sub>2</sub>O left on the catalyst surface. One possibility is that adsorbed H<sub>2</sub>O comes off the catalyst surface ( $\text{H}_2\text{O}-\text{s} = \text{H}_2\text{O} + \text{s}$ , where s represents a vacant site), and simultaneously enters the gas phase. This is consistent with the above discussion in view of the observation from Fig. 3a. Another possibility is that the remaining adsorbed H<sub>2</sub>O oxidizes an active metal site and H<sub>2</sub> is released simultaneously ( $\text{H}_2\text{O}-\text{s} + \text{M} = \text{H}_2 + \text{O}-\text{s}-\text{M}$ , where M represents the active metal site). It might be that the deoxidization of the adsorbed H<sub>2</sub>O is enhanced by a temperature increase, resulting in a monotonic increase of the H<sub>2</sub> signal between 513 and 573 K. It is not surprising that the amount of H<sub>2</sub> is decreased beyond 573 K, because the concentration of the adsorbed water is low and decreases with increasing temperatures between 573 and 773 K (Fig. 3a). Thus, the result of the TPSR of H<sub>2</sub>O and CO further shows that the redox mechanism is the most possible pathway on the NBC-1 surface.

#### 4. Conclusions

The NBC-1 catalyst is an active and thermo-stable Cr-free iron-based catalyst for the high-temperature WGS reaction. Its activity and thermal-stability are comparable to those of the commercial C12-4 Fe-Cr catalyst. It is a good alternative to traditional Fe-Cr WGS catalysts. Iron in the fresh NBC-1 catalyst is present as  $\gamma\text{-Fe}_2\text{O}_3$ . During reduction and reaction, most of the  $\gamma\text{-Fe}_2\text{O}_3$  in the catalyst

is transformed to the Fe<sub>3</sub>O<sub>4</sub> with perfect structure. It is postulated that Fe<sub>3</sub>O<sub>4</sub> acts as active phase for WGS reaction. Desorption of the CO<sub>2</sub>, CO and H<sub>2</sub>O adsorbed on the NBC-1 surface takes place at different temperature ranges. Less than 300 °C is required for the CO and CO<sub>2</sub> and over 400 °C for the H<sub>2</sub>O. Under reaction conditions (>350 °C), the adsorbed H<sub>2</sub>O reacts with CO to produce H<sub>2</sub> and CO<sub>2</sub>. It is proposed that the redox regenerative mechanism is a dominant pathway for the WGS reaction on the NBC-1 catalyst.

#### Acknowledgements

Financial supports from the Natural Science Foundation of China (20066002) and the Science Foundation of Inner Mongolia (20041001) are greatly acknowledged. We are grateful to Profs. T.L. Diao and H.F. Jin for valuable discussions on preparation of the paper.

#### References

- [1] D.S. Newsome, Catal. Rev. Sci. Eng. 21 (1980) 275.
- [2] C. Rhodes, B.P. Williams, F. King, Catal. Commun. 3 (2002) 381.
- [3] G.C. Chinchin, Euro Patent, A-0 062410 (1982).
- [4] G.C. Chinchin, M.S. Spencer, K.C. Waugh, J. Chem. Soc. Faraday Trans. 183 (1987) 2193.
- [5] J. Ladebeck, K. Kochloeff, Stud. Surf. Sci. Catal. 91 (1995) 1079.
- [6] M.L. Kundu, A.C. Sengupta, G.C. Maiti, J. Catal. 112 (1988) 375.
- [7] Y.G. Shirokov, Khim. Khim. Tekhnol. 21 (1978) 1339.
- [8] D.G. Rethwisch, J.A. Dumesic, Appl. Catal. 21 (1986) 97.
- [9] J. Tsagaroyannis, K.J. Haralambous, Z. Loizos, Mater. Lett. 28 (1996) 393.
- [10] G.C. de Araujo, M. do Carmo Rangel, Catal. Today 62 (2000) 201.
- [11] T. Bunluesin, Appl. Catal. B 15 (1998) 107.
- [12] X. Wang, R.J. Gorte, J.P. Wagner, J. Catal. 212 (2002) 225.
- [13] X.M. Qi, M. Flytzani-Stephanopoulos, Ind. Eng. Chem. Res. 43 (2004) 3055.
- [14] C. Padeste, N.W. Cant, Catal. Lett. 18 (1993) 305.
- [15] A. Trovarelli, Catal. Rev. Sci. Eng. 38 (1996) 439.
- [16] Y. Hu, H. Jin, D. Hao, Chem. Eng. J. 78 (2000) 147.
- [17] G. Parravano, Ind. Chem. Eng. 49 (1967) 266.
- [18] H. Jin, Q. Liu, Z. Mu, L. Diao, X. Zhang, W. Ma, Chin Patent, ZL95 121834.4 (1999).
- [19] T. Taniyama, Y. Kitamoto, Y. Yamazaki, J. Appl. Phys. 89 (2001) 7693.
- [20] D.P.E. Dickson, F. Berry, Mössbauer Spectroscopy, Cambridge University Press, UK, 1986, p. 169.
- [21] M. Tinkle, J.A. Dumesic, J. Catal. 103 (1987) 65.
- [22] G.C. Chinchin, M.S. Spencer, J. Catal. 112 (1988) 325.